Numerical Modelling of Deformation Behaviour of Dry-Stack Stone Masonry

by

R SENTHIVEL, P B LOURENCO and G VASCONCELOS
Department of Civil Engineering, School of Engineering, Azurem Campus
University of Minho, P-4800-058 Guimaraes, Portugal

ABSTRACT
The behaviour of masonry under monotonic and cyclic loading is of vital interest for engineering of masonry structures. The response parameters measured under monotonic and cyclic loading including the ductility, strength deterioration, stiffness degradation and energy dissipation capacity provide the basis for evolving the design criteria. A numerical simulation based on experimental test data has been carried out to model the monotonic and reversed cyclic load-displacement hysteresis curves of dry-stack mortarless sawn stone masonry using a multi-surface interface model where stone units and joints are assumed elastic and inelastic respectively. Finite element software, Diana version 8.1, has been employed to carry out the present numerical modelling. The stone units were modelled using eight node continuum plane stress elements with Gauss integration and the joints were modelled using six node zero thickness line interface elements with Lobatto integration. This paper describes the experimental research work and details of numerical modelling carried out and reports the numerical monotonic load-displacement curve and reversed cyclic load-displacement hysteresis curves.

NOTATION

$K_{n,\ joint}$ = Normal joint stiffness
H = Height of stone
E_{wall} = Young's modulus of wall
E_{stone} = Young's modulus of stone
$K_{s,\ joint}$ = Tangential stiffness
$K_{n,\ joint}$ = Normal joint stiffness
μ = Poisson's ratio

1. INTRODUCTION

Dry stone masonry is the most ancient, durable, widespread, and environmentally friendly building method devised by mankind. Stone structures built without mortar rely on the skill of the craftsmen and the forces of gravity and frictional resistance. Stone has been a successful building medium throughout the ages and around the world because of its unique range of benefits. The structures are remarkably durable; indeed, if correctly designed, they are earthquake resistant. They resist fire, water, and insect damage. The mason needs a minimum of tools; the work is easily repaired; the material is readily available and recyclable. Dry stone masonry does not deplete resources and, aesthetically, complements and enhances the landscape. Archaeologists have determined that the Chinese built dry stone terraces at least 10,000 years ago. In Britain, ancient tribes built dry stone shelters just after the last ice age, 8,000 years ago. High quality stone tools recently found in Europe are 2.2 million years old. In addition to the neglect and destruction of historic structures, the craft is handicapped by lack of technical information and lack of skilled preservation personnel. Construction and engineering data that professionals need are scarce and, if recorded at all, are difficult to locate. A large number of historical buildings in Portugal are built with stone with or without mortar. The primary function of masonry elements is to sustain vertical gravity load. However, structural masonry elements are required to withstand combined shear, flexure and compressive stresses under earthquake or wind load combinations consisting of lateral as well as vertical loads.

A research program was carried out by Vasconcelos (2005) at the University of Minho to experimentally evaluate the in-plane seismic performance of ancient sawn dry stack masonry without bonding mortar. Monotonic and reversed cyclic loading tests with varying pre-compression were performed to investigate the strength, deformation capacity, monotonic and cyclic load-displacement hysteresis response and stiffness characterization. The data obtained from the above experimental research has been used as a base for the present numerical simulation. The simulation was carried out using a multisurface interface model where stones and joints are assumed elastic and inelastic respectively. The stones were modelled using an eight node continuum plane stress elements with Gauss integration and the joints were modelled using a six node line interface elements with Lobatto integration. This paper presents outline of the experimental research work and details of numerical modelling carried out and reports the numerical monotonic load-displacement curves, reversed cyclic load-displacement hysteresis curves and conclusions.

2. OUTLINE OF EXPERIMENTAL RESEARCH WORK

The main object of the experimental research work [Vasconcelos (2005)] was to evaluate the seismic performance of dry stack masonry shear walls found in ancient masonry structures. A typical dry stacked mortarless sawn stone masonry test specimen is shown in Figure 1. The dimension of the sawn stone was 200mm (length) x 150mm (height) x 200mm (width) and the dimension of test specimen was 1000mm (length) x 1200mm (height) x 200mm (width), and the height to length ratio was 1.2. Static monotonic and reversed cyclic tests were carried out with three distinct pre-compressions levels such as 100kN (σ_0 = 0.5N/mm^2), 175kN (σ_0 = 0.875N/mm^2) and 250kN (σ_0 = 1.25N/mm^2) using the experimental set-up shown in Figure 2. The base of the wall was fixed to the reaction slab through a couple of steel rods and the pre-compression load was applied through top vertical actuator. A stiff steel beam was used to distribute the vertical pre-compression loading and a set of steel rollers were placed between the test specimen and the top stiff steel beam to allow relative horizontal displacement due to the imposed lateral load or displacement with respect to the vertical actuator. The seismic action was simulated by imposing incremental static lateral displacement history shown in Figure 3. The deformation of the wall was measured by means of needle type Linearly Variable Differential Transducers (LVDTs).

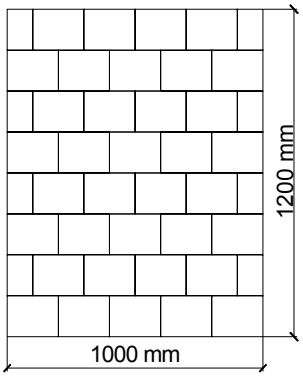

Figure 1 Details of experimental test specimen

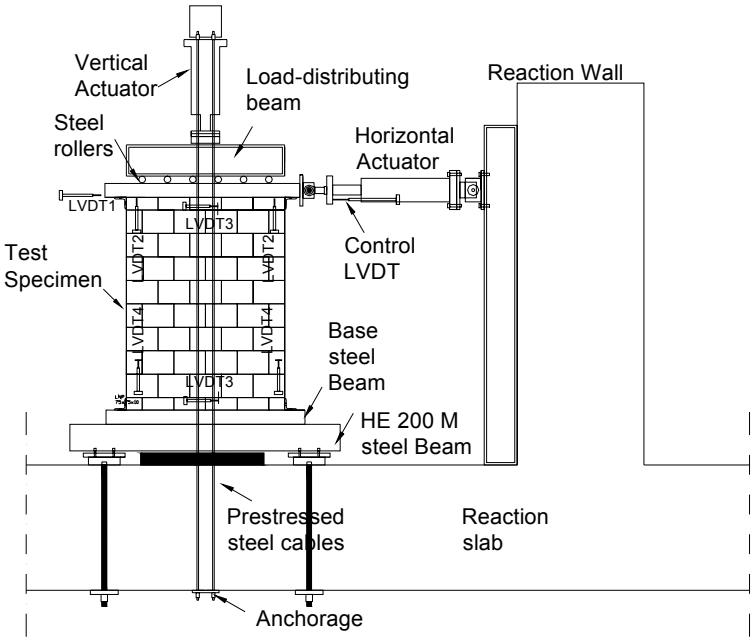

Figure 2 Experimental test set up and position of LVDTs

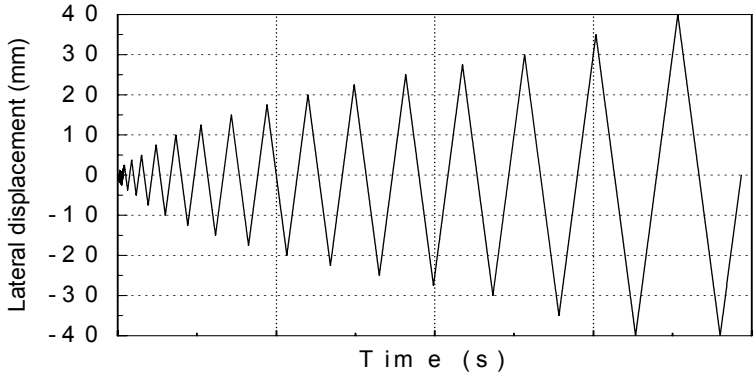

Figure 3 Displacement history

3. DETAILS OF NUMERICAL MODELLING

The data obtained from the above experimental research carried out by Vasconcelos (2005) has been used as a base for the present numerical analysis/ simulation. A non-linear finite element analysis has been carried out using the DIANA (version 8.1) software. The simulation was carried out using a multi-surface interface model where stones and joints are assumed elastic and inelastic respectively. The stones were modelled using an eight node continuum plane stress elements (Figure 4) with Gauss integration and the joints were modelled using a six node and zero thickness line interface elements (Figure 5) with Lobatto integration proposed by Lourenco and Rots (1997). Figure 6 shows the combination of stone and interface model.

The present interface material model is also know as the 'Composite Interface model', is appropriate to simulate fracture, frictional slip as well as crushing along material interfaces, for instance at joints in masonry. Usually the brick units are modelled as linear elastic, or viscoelastic continua, while the mortar joints are modelled with interface elements, which obey the nonlinear behaviour described by the following combined cracking-shearing-crushing model (Lourenço and Rots [1997]). In some cases it is justified to model also the mortar with continuum elements, and the interface elements and material behaviour are employed to capture the physical interface between bricks and mortar (Figure 7a).

The finite element mesh was generated using an external masonry pre-processor called make wall developed by Lourenço (1996b) and the run-command is make_wall mesh.dat. Size of the unit is 200mm (length) × 150mm (height) × 200mm (thickness) and joint thickness is zero.

Dry stone masonry exhibits a peculiar "elastic" behaviour under compressive loading [Vasconcelos (2005)]. The average value of Young's modulus based on 10 monotonic uniaxial compressive tests performed on cylindrical specimens was 15500N/mm^2. Young's modulus of stone prisms built with four stacked stones and subjected to uniaxial compression reads 14800N/mm^2 (average of 4 prisms result). The Young's modulus of the stone was fixed as 15500N/mm^2 in the present micro-modelling simulation. Young's modulus of large walls is considerably different from the Young's modulus measured in small test specimens. This phenomenon has been found and reported by Lourenço (1996) from the modelling of masonry shear walls tested at the Eindhoven University of Technology. The reason for the difference in stiffness between large and small specimens is because of poor alignment in case of large specimens.

Normal joint stiffness ($K_{n,\ joint}$) was calculated using the following formulation proposed by Lourenco (2006a) in which the wall is consider as a series of two spring in vertical direction, one representing a stone and the other representing a joint.

$$K_{n,\ joint} = 1/(h(1/E_{wall} - 1/E_{stone})) \quad (1)$$

Where

$K_{n,\ joint}$ = Normal joint stiffness
h = Height of stone (150mm)
E_{wall} = Young's modulus of wall
E_{stone} = Young's modulus of stone

The tangential stiffness ($K_{n,\ joint}$) was calculated directly from the normal stiffness using the theory of elasticity as follows, Lourenco (2006a):

$$K_{s,\ joint} = K_{n,\ joint}/\ 2(1+v) \quad (2)$$

Where

$K_{s,\ joint}$ = Tangential stiffness
$K_{n,\ joint}$ = Normal joint stiffness
V = Poisson's ratio (0.2)

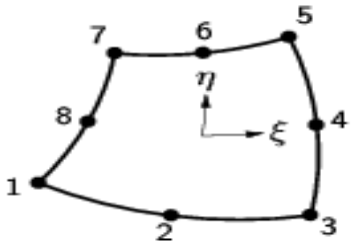

Figure 4 Typical eight nodes continuum plane stress element (CQ16M)

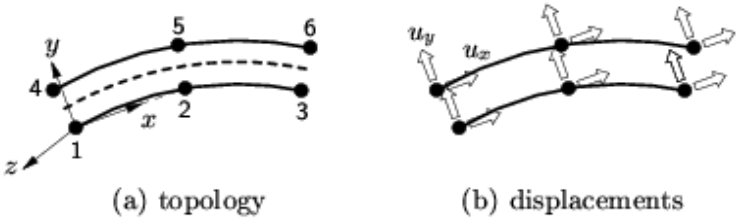

Figure 5 Typical six node zero thickness line interface elements (CL12I)

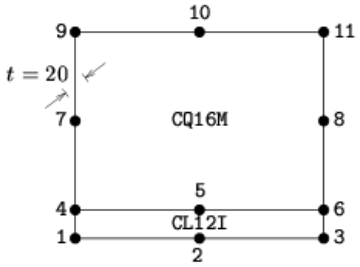

Figure 6 Typical combined CQ16M and CL12I element model

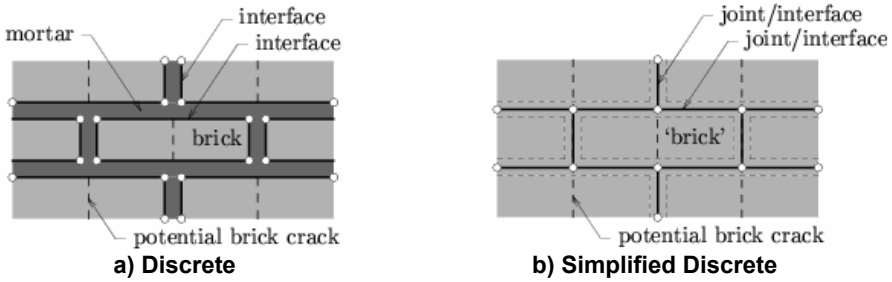

a) Discrete **b) Simplified Discrete**

Figure 7 Modelling techniques for masonry

The tensile strength and cohesion of the joints are assumed as zero. An experimental study on similar stone was carried out by Ramos (2001) found the tensile strength of stone is 3.7N/mm^2 and fracture energy is 0.11Nmm/mm^2. In addition, Lourenco and Ramos (2004) found the values for tanφ (0.6) and tanψ (0) where φ is friction angle and ψ is dilatancy angle of the stone joints. The uniaxial compressive strength of stone assembly was found equal to 57N/mm^2. The fracture energy in compression was assumed to be half of the value given by Model Code 90 (CEB-FIB, 1990) for concrete, due to the higher brittleness of stone.

This section deals with syntax of the nonlinear material input for the composite interface model. The model sets a nonlinear relation between tractions (i.e. stresses) and relative displacements across the interface. The tractions are a normal traction t_n and a shear traction t_t . The relative displacements are a normal displacement Δu_n and a shear displacement Δu_t . Masonry inelastic behavior may be specified according to the following syntax:

'MATERI'
COMBIF
GAPVAL *ft$_r$*
MO1VAL *gf1$_r$*
FRCVAL *ch$_r$ phi$_r$ psi$_r$ [phi$_r$, sigu$_r$, delta$_r$]*
MO2Val *[gf2a$_r$] gf2b$_r$*
CAPVAL *fc$_r$ cs$_r$*
MOCVAL *gfc$_r$ kp$_r$*

Where, COMBIF indicates the use of the multi-surface interface yield criterion for combined cracking-shearing-crushing. GAPVAL (*ft$_r$*) is the tensile strength f_t., MO1VAL (*gf1*) is the fracture energy G_f^I for Mode-I. FRCVAL describes the friction criterion: *ch* is the cohesion *c*, *phi* is the tangent of the friction angle, and *psi* is the tangent of the dilatancy angle. Variable friction and dilatancy requires three more parameters: *phir* is the residual friction coefficient, *sigu* is the confining normal stress, σ_u for which the dilatancy coefficient is zero, and *delta* is the exponential degradation coefficient δ of the dilatancy coefficient with shear-slipping displacement. In this case the specified *phi* and *psi* will be considered as initial values. MO2VAL defines the Mode-II fracture energy G_f^{II}: *gf2a* and *gf2b* are the factors *a* and *b* in $G_f^{II} = a\sigma + b$. If a factor is not specified, this will be taken as zero by default, [a = 0] and G_f^{II} will be constant. CAPVAL describes the cap criterion: *fc* is the compressive strength f_c and *cs* is factor C_s which controls the shear traction contribution to compressive failure. MOCVAL describes the compressive inelastic law: *gfc* is the compressive fracture energy G_{fc} and *kp* is the equivalent plastic relative displacement *kp* corresponding to the peak compressive stress. The necessary input parameters such as elastic, inelastic and strength data required for the present analysis was are extracted from the experimental research work done by Vasconcelos (2005) and Oliverira (2003).

3. NUMERICAL ANALYSIS TEST RESULTS AND DISCUSSION

Figure 8 presents the numerical finite element model before deformation. Figure 9a – 9c presents the shape of the total deformed mesh under monotonic loading with different level of pre-compression loading conditions such as 100, 175 and 250kN. Rocking failure was observed for lower level of pre-compression (100 and 175kN) and rocking with toe crushing failure was observed for higher level of pre-compression (250kN). The observed failure mode is in good correspondence with the experimental failure mode presented in the Table 1. Figure 9d presents shape of the incremental deformed mesh at ultimate lateral load/ displacement for 250kN pre-compression load.

The monotonic load and corresponding displacement obtained from the numerical analysis has been plotted. The Numerical load-displacement curves and experimental load-displacement curves are compared and presented in Figure 10a-10c. A good correspondence between numerical and experimental response has been found for all three cases of pre-compression levels. The cyclic load and corresponding displacement obtained from the numerical analysis has been plotted and presented in Figure 11. The numerical model used in this study produces adequate results for monotonic loading but it is not capable of predicting the experimental cyclic behaviour accurately, due to inadequate crack closure.

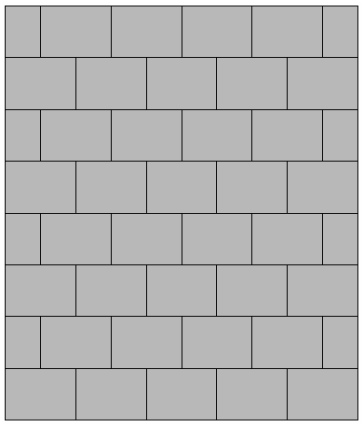

Figure 8 Model before deformation

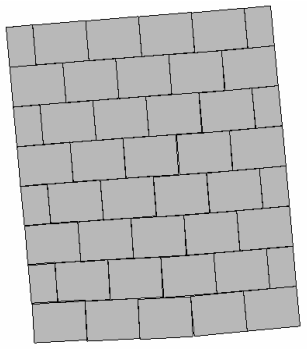

Figure 9a Deformed shape (for pre-compression 100kN)

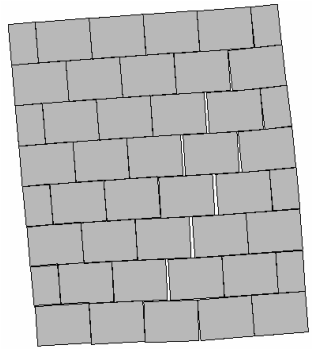

Figure 9b Deformed shape (for pre-compression 175kN)

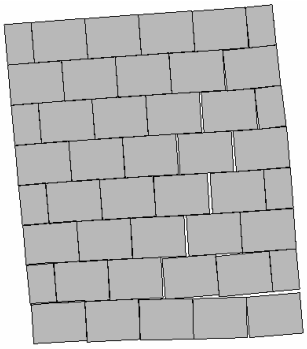

Figure 9c Deformed shape (for pre-compression 250kN)

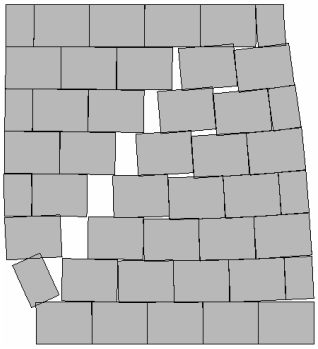

Figure 9d Incremental deformed shape at collapse (for pre-compression 250kN)

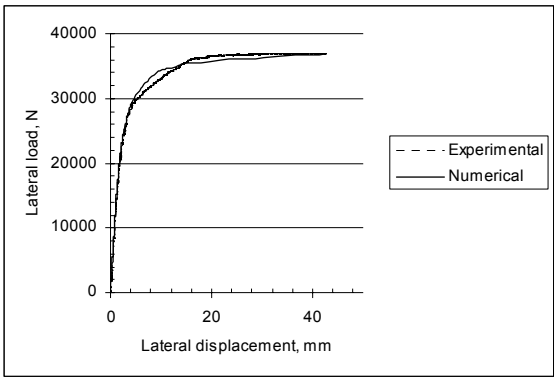

Figure 10a Load-displacement curve for pre-compression 100kN

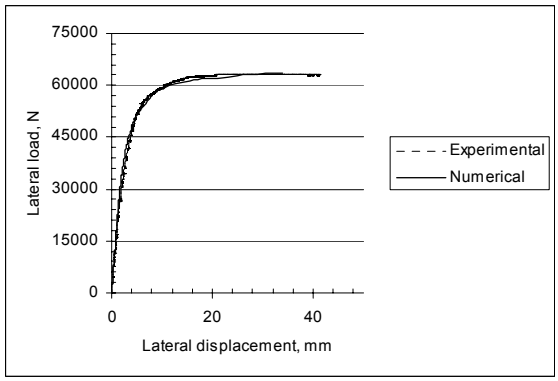

Figure 10b Load-displacement curve for pre-compression 175kN

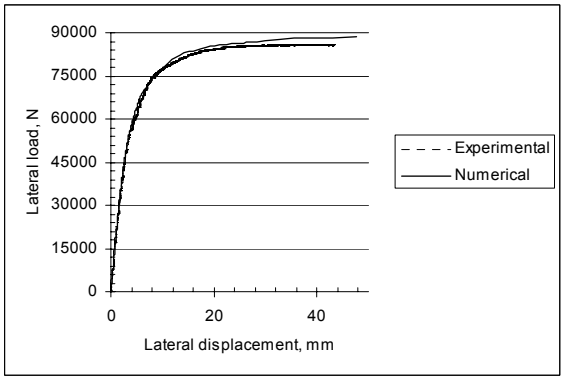

Figure 10c Load-displacement curve for pre-compression 250kN

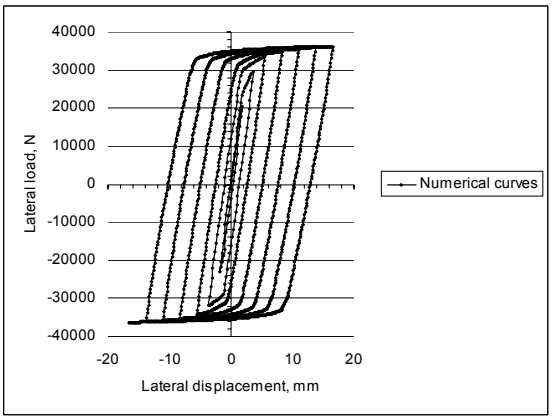

Figure 11a Numerical cyclic load-displacement hysteresis curves

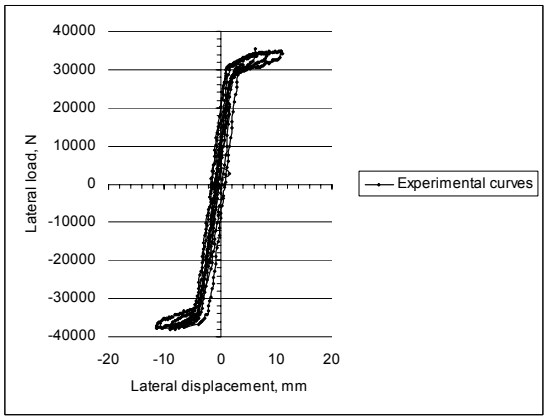

Figure 11b Experimental cyclic load-displacement hysteresis curves

Table 1
Experimental failure modes

Vertical pre-compression (kN)	Failure mode
100	Rocking/ Rocking and toe crushing
175	Rocking/ Rocking and toe crushing
250	Rocking and toe crushing

4. SUMMARY AND CONCLUSIONS

The main object of the present numerical analysis/ simulation is to evaluate the seismic performance of dry stack masonry shear walls found in ancient masonry structures. A non-linear finite element analysis has been carried out using the DIANA (version 8.1) software. The simulation was carried out using a multi-surface interface model where stones and joints are assumed inelastic and elastic respectively. The stones were modelled using eight node continuum plane stress elements with Gauss integration and the joints were modelled using six node and zero thickness line interface elements with Lobatto integration proposed by Lourenco and Rots (1997). Elastic, inelastic and strength parameters have been extracted and calculated based on the experimental research test data. The co-efficient of friction between stone unit surfaces and its contribution to the lateral resistance has been discussed in detail by Vasconcelos (2005) and Oliverira (2003).

Rocking failure was observed for lower levels of pre-compression and rocking with toe crushing failure was observed for higher levels of pre-compression. The failure mode observed is in good agreement with the experimental failure modes. The load and corresponding displacement obtained from the numerical analysis has been plotted. The numerical load-displacement curves and experimental load-displacement curves are compared and presented. A good correspondence between numerical and experimental response has been found for all the pre-compression levels tested.

The cyclic load and corresponding displacement obtained from the numerical analysis has been plotted. The numerical model used in this study produced better results for monotonic loading but it is not capable of predicting the experimental cyclic behaviour accurately. The main disadvantage with the present model is that the bed joint opening does not close on release of the lateral cyclic load or displacement. An attempt has been under way to use another approach called a friction model to predict more accurately the experimental cyclic load-displacement hysteresis curves.

REFERENCES

1. OLIVEIRA, D. *Experimental and numerical analysis of block masonry structures under cyclic loading*, Ph.D. Thesis, University of Minho, Portugal, 2003. Available at www.civil.uminho.pt/masonry.
2. RAMOS, L F. *Experimental and numerical analysis of historical masonry structures*, Msc Thesis, University of Minho, 2001 (in Portuguese). Available at www.civil.uminho.pt/masonry.
3. VASCONCELOS, G F. *Experimental Investigations on the Mechanics of Stone Masonry: Characterization of Granites and Behavior of Ancient Masonry Shear Walls*, PhD Thesis, University of Minho, Portugal, 2005. Available at www.civil.uminho.pt/masonry.
4. LOURENÇO, P B. *Computational strategies for masonry structures*, Ph.D. Dissertation, Delft University of Technology, Delft, 1996.
5. LOURENÇO, P B. A user/programmer's guide for the micro-modelling of masonry structures. Relatório nº 03.21.1.31.35, Universidade Técnica de Delft, Delft, Países Baixos e Universidade do Minho, Guimarães, 50, 1996.
6. LOURENÇO, P B and ROTS, J G. A multi-surface interface model for the analysis of masonry structures. J. Struct. Eng., ASCE **123**, (7), 660-668, 1997.
7. LOURENÇO, P B and RAMOS, L F. Characterization of the cyclic behaviour of dry joints, J. Struct. Eng., ASCE, **130**, (5), pp. 779-786, 2004.
8. MC90, *CEB-FIB Model Code 1990 for concrete structures*, CEB Bulletin d'Information, No.213/214, Comité Euro Interantional du Béton, Lausanne, 1993.
9. Diana v8. 2000. *User's Manual*, TNO Company, The Netherlands, 2000, www.tnodiana.com.